

Modelling plausible scenarios for the Omicron SARS-CoV-2 variant from early-stage surveillance

Christopher J. Banks¹, Ewan Colman¹, Anthony Wood¹, Thomas Doherty², and Rowland R. Kao^{1,3,*}

¹Roslin Institute, University of Edinburgh

²Department of Mathematics and Statistics, University of Strathclyde

³Royal (Dick) School of Veterinary Studies, University of Edinburgh

*Correspondence: rowland.kao@ed.ac.uk

November 28, 2022

Abstract

In this paper we used an adapted version of an existing simulation model of SARS-CoV-2 transmission in Scotland to investigate the rise of the Omicron variant of concern, in order to evaluate plausible scenarios for transmission advantage and vaccine immune escape relative to the Delta variant. We also explored possible outcomes of different levels of imposed non-pharmaceutical intervention. The initial results of these scenarios were used to inform the Scottish Government in the early outbreak stages of the Omicron variant.

We use an explicitly spatial agent-based simulation model combined with spatially fine-grained COVID-19 observation data from Public Health Scotland. Using the model with parameters fit over the Delta variant epidemic, some initial assumptions about Omicron transmission advantage and vaccine escape, and a simple growth rate fitting procedure, we were able to capture the initial outbreak dynamics for Omicron. We also find the modelled dynamics hold up to retrospective scrutiny.

We found that the modelled imposition of extra non-pharmaceutical interventions planned by the Scottish Government at the time would likely have little effect in light of the transmission advantage held by the Omicron variant and the fact that the planned interventions would have occurred too late in the outbreak's trajectory. Finally, we found that any assumptions made about the projected distribution of vaccines in the model population had little bearing on the outcome, in terms of outbreak size and timing, rather that the detailed landscape of immunity prior to the outbreak was of far greater importance.

1 Introduction

The B.1.1.529 SARS-CoV-2 variant was first detected in South Africa and reported to the World Health Organisation on 24th November 2021; it was designated the Omicron variant of concern (VOC) two days later [1]. The first cases of Omicron were detected in Scotland around 29th November [2]. Globally Omicron was associated with rapid spread and increase in case numbers, most likely due to some combination of increased transmission potential and increased vaccine escape [3]. However greater infectiousness was somewhat offset by a reduction in outcome severity.

Upon the introduction of the variant to Scotland there was an urgent need to understand how the dynamics of transmission may be affected and how this in turn would affect outcomes and local levels of pressure on the National Health Service. It was also necessary to estimate the effect of control measures.

In this study we used an adapted version of an existing simulation model of SARS-CoV-2 transmission in Scotland, SCoVMod [4], to investigate the rise of the Omicron VOC, in order

to evaluate plausible scenarios for transmission advantage and vaccine immune escape relative to the Delta VOC. We explored possible outcomes of different levels of imposed non-pharmaceutical interventions (NPI's) and booster vaccination, in order to provide insight into the possible severity of the epidemic in terms of the probable number of infections.

Using the SCoVMod simulation model, we fit model parameters to the explicit pattern of recorded cases across all local authorities in Scotland, considering the period from August to December 2021. This was a period in which the Delta VOC was dominant and over which the COVID-19 epidemic in Scotland can be considered as a single infection process. We introduced a variant infection (representing the Omicron VOC), and then modelled the period from the 11th December to the end of March 2022. At time of writing there is considerable information on the differences between Omicron and Delta. However we assume knowledge only available up to 11th December when this analysis was initiated, to demonstrate an analytical approach that is relevant to that point in spread of Omicron. Because this was a period of sustained consistent exponential growth, with no obvious change in interventions, this also allows us to fit a single model assuming a single transmission rate. We examine a range of scenarios with either fixed parameters or multipliers of the Delta parameters for the variant process.

In order to fit the model to observed data our simulated epidemics are compared to the spatio-temporal pattern of COVID-19 incidence in Scotland. Non-observable parameters were estimated using the number of infections estimated in the population. Incidence of SARS-CoV-2, here defined as the number of new infections each day, is not directly obtainable from surveillance data and therefore needs to be estimated. The number of confirmed cases found through PCR and lateral flow device tests is a useful indicator of incidence, however, a large proportion of infections are not ascertained through these methods [5].

At local scales it is not appropriate to apply the same ascertainment rate to all sub-regions. This is particularly true in a heterogeneous population like Scotland where infection levels, access to testing, and test seeking propensity vary greatly between local authority areas. Hence we also introduce a novel method to estimate the incidence in each sub-region of Scotland. We derive a formula that takes the number of positive and negative PCR tests across the nation as input, and gives an estimate of the number of people testing positive for SARS-CoV-2 in each sub-region on any given day. The formula is derived from assumptions about the relationship between infection prevalence and observed test data. We then re-scale the prevalence estimate to form our estimate of incidence. The result of which is used as our observed incidence in the model-fitting process.

This study is similar in scope to other early-response scenario models, for example both Barnard et al. [6] and Keeling et al. [7]. However, we focus on Scotland and implement a more detailed individual based model, including explicit inter-location mobility, and with finer grained data resolution. We make similar assumptions on vaccine efficacy and escape.

The initial results of these scenarios were used to inform the Scottish Government and intended to aid policy decision making in the early outbreak stages of the variant [8].

2 Methods

2.1 Data

Data for fitting Delta, estimating the seeding of Omicron, and the distribution of COVID-19 vaccines was supplied by Public Health Scotland's eDRIS team [9]. We differentiate between Delta and Omicron using S-Gene Target Failure (SGTF) in PCR tests as a proxy for Omicron infections. Community tests where SGTF is measured represent approximately 80% of all tests at the time of running these scenarios. We also used publicly available Scottish census data from National Records for Scotland (NRS) [10]. We used datazone (DZ) level resolution where DZs are population census units of approximately 500 to 1,000 residents. The data for assignment of individuals to work locations is drawn from the NRS Census Flows data [11], Table WU01UK, which provides origin/destination workplace data for the population from the 2011 census. We adjust these with respect to the 2018 population estimates.

Age demographics and movement to work patterns are available at the level of Census Output Areas (OA), each of which contains approximately 20 households or 50 people [12]. Census data on the Scottish Index of Multiple Deprivation (SIMD) [13] considers multiple relative deprivation measures and combines them into a single value. Deprivation data are publicly available at the DZ level.

We also used publicly available data from Google to estimate mobility levels over time, with respect to commuting patterns [14].

2.2 Model

SCoVMod is an explicitly spatial agent-based simulation model that accounts for recorded commuter patterns and additional local movements that are intended to capture non-work interactions such as recreation, shopping, and school. These movements are further modulated by the recorded time-varying mobility statistics, and geographically explicit population age structures. Whilst this does not capture all human movement, we assume that commuting patterns capture a large proportion of the long-range mobility and that local movements at least partially capture the non-commuting population travelling to shops, schools, and other local community movements. This is a similar assumption regarding mobility to the one used in other studies, including e.g. Barnard et al. [6]. The model also uses deprivation metrics to account for spatial heterogeneity in outcome likelihoods. The model is parameterised against an estimation of the number of COVID-19 infections according to the observed number of COVID-19 reported cases in each Council Area, using a model for the case ascertainment ratio [5]. The model parameters were inferred using Approximate Bayesian Computation (ABC) [15].

The core of the simulation model breaks down into the following parts:

- Local transmission—a homogeneous mixing compartmental model for each OA of the country;
- National transmission—a network-based simulation of the movement of individuals between OAs;
- Parameter inference—a Bayesian estimation of the parameters for local transmission, this also involves a model of infection incidence used as the observed value for inference;
- Transmission rate over time adjustment—the modulation of both local and national transmission to simulate non-pharmaceutical interventions and other changes in transmission rates over time.

The compartmental model considers key aspects of COVID-19 epidemiology including phases for latent infection, infectious and mildly infected (showing few or no clinical signs) and severely infected (with substantial clinical signs) individuals, hospitalised, recovered and died, similar to other investigations [16, 17]. These epidemiological processes are captured as individual disease states (Figure 1). Individuals are also stratified into three age groups: young (0–15), adult (16–64) and elderly (65+). Within-OA transmission is assumed to be homogeneously mixed while between-OA transmission is determined by the empirical age-specific patterns of home and work contact (creating day/night patterns of contact). We do not consider overnight shifts in location or introductions from outside Scotland beyond the impact on the initial seeding.

Deprivation is also known to influence COVID-19 transmission. We therefore adjust transmission rates in the model with the average health index in the local council area.

Population mobility patterns are determined by the patterns of movements to work recorded in Scottish Census data. We assume that only adults contribute to commuter movement, in the daytime; the remaining proportion of adults and all young and elderly individuals are assumed to move primarily within their local OAs, which also account for non-work activities. Finally, commuting in the model is restricted to healthy and exposed or mildly symptomatic individuals; severely infected and hospitalised individuals do not commute. The day/night patterns also result in two transmission rates.

Local transmission (within-OA)

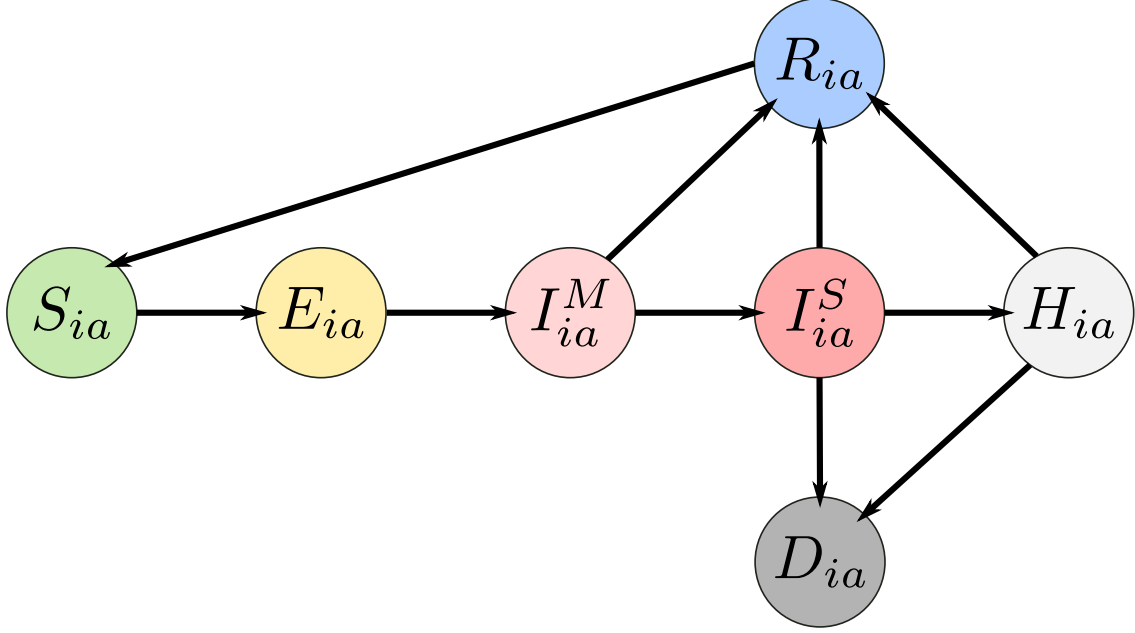


Figure 1: Schematic of infection stages in SCoVMod. Individuals pass through stages post infection as described by arrows. Not all stages are obligatory for all infected individuals (e.g. some individuals recover without going to hospital).

Within each OA (i) the infection process is governed by a compartmental model (Figure 1) for which the frequency dependent force of infection $\Lambda_i(t)$ defined in Figure S1. In the compartmental model are infection classes S (susceptible), E (exposed), I^M (mildly infected), I^S (severely infected), H (hospitalised).

The state transitions in the model are described by the following equations:

$$\begin{aligned}
 \frac{dS_{ia}}{dt} &= -\Lambda_i(t)\beta_{CA}S_{ia} + \nu R_{ia} \\
 \frac{dE_{ia}}{dt} &= \Lambda_i(t)\beta_{CA}S_{ia} - \gamma E_{ia} \\
 \frac{dI_{ia}^M}{dt} &= \gamma E_{ia} - (\gamma_M + \rho_M)I_{ia}^M \\
 \frac{dI_{ia}^S}{dt} &= \gamma_M I_{ia}^M - (\rho_{Sa} + \mu_{Sia} + \eta)I_{ia}^S \\
 \frac{dH_{ia}}{dt} &= \eta I_{ia}^S - (\rho_{Ha} + \mu_{Hia})I_{ia}^S \\
 \frac{dR_{ia}}{dt} &= \rho_M I_{ia}^M + \rho_{Sa} I_{ia}^S + \rho_{Ha} H_{ia} - \nu R_{ia} \\
 D_{ia} &= N_{ia} - (E_{ia} + I_{ia}^M + I_{ia}^S + H_{ia} + R_{ia})
 \end{aligned}$$

The force of infection, Λ , is detailed in Figure S1 and other state transition rates are given by: γ for $E \rightarrow I^M$, γ_M for $I^M \rightarrow I^S$, η for $I^S \rightarrow H$, ρ_M for $I^M \rightarrow R$, ρ_{Sa} for $I^S \rightarrow R$ for age class a , ρ_{Ha} for $H \rightarrow R$ for age class a , μ_{Sia} for $I^S \rightarrow D$ for age class a and location i , μ_{Hia} for $H \rightarrow D$ for age class a and location i , and ν for $R \rightarrow S$.

Transmission rates are adjusted by location, according to SIMD Health Index:

$$\beta_{CA} = 1 + (\beta_{mod}(k_{CA} - k_{av}))$$

where β_{CA} is the transmission modifier rate for a given CA, k_{CA} is the CA mean health index value (from the SIMD), and β_{mod} is a fitted parameter for the strength of the overall effect.

For this study the model is extended with a second strain (variant) of the virus. The compartment structure remains the same, but individuals can be infected with one of two strains, each with a different set of rates. We assume complete cross immunity between strains.

The values for all parameters are either established from the literature (Table S1) or fit (see below).

National transmission (between-OA movements)

Between OAs individuals move daily across a network of locations defined by Scottish Census data adjusted by Google mobility data.

From the current population estimates we draw the number of individuals whose primary residence is mapped onto an OA, with their age group. The total population of Scotland from this estimate is 5,438,054 (Young: 919,580; Adult: 3,492,421; Elderly: 1,026,053). Of the adults 1,960,712 commute to work, reduced to 647,034 under lockdown (see details below).

An individual’s workplace is assigned by distributing a proportion of the population of each location to each work location, weighted by the proportion of individuals from each home location in the census flows data who work in another location. For the remaining proportion we synthetically generated daytime locations by randomly selecting OAs either from the OAs within the same intermediate zone (a geographical area containing approximately 4200 people), with probability 0.9, or from the OAs within a neighbouring intermediate zone, with probability 0.1.

For each origin o and destination d we assign a weight w_{od} from the census flow data:

$$w_{od} = \frac{n_{od}}{t_o}$$

where n_{od} is the total number of people who move from o to d to work, and t_o is the total number who move from origin o to any location for work. We take the individuals of each home location if they are eligible to work (total n_o); in this case we assume all individuals of adult age 16–64. Each destination is assigned to $n_o \times w_{od}$ of these individuals. The individuals who remain have no assigned workplace—we assume either they do not work, or they work within their home location.

For each day of the simulation we consider two time steps: a day step where individuals can move to their place of work, and a night step where those individuals move back to their home location. In each day step, we take each destination location d . Let λ_d be the number of eligible workers who may move to the destination location. The number of moves s is then scaled according to the per cent change in mobility m (see below) for the given day: $s_m = \lfloor s(1 + \frac{m}{100}) \rfloor$.

In order to improve the computational efficiency of the overall simulation, movements of commuters between OAs were batched into groups of 5, with movements between OAs of fewer than five individuals per day retained at a proportionate rate by drawing from a binomial distribution: $s_{mt} \sim B(s_m, \frac{1}{5})$. If the sampled number of workers s_{mt} is less than or equal to the number of workers who may normally move to destination d , then those who move are sampled randomly from those who may normally move. However, if s_{mt} is greater than the number of workers who may normally move to d , then the additional workers are drawn randomly from workers who have no assigned destination location. While this reduces the overall network link density, the effect on transmission dynamics in this setting is negligible. We note that this means that interpretation of the combined β_D and β_N must be made with caution and not compared directly to other models.

For each night of the simulation, the workers who moved in the day step are moved back to their origin location.

Vaccination

Vaccination is represented in the model by flagging an individual with its vaccination status. The transmission rates affecting a vaccinated individual are adjusted accordingly—i.e. the probability that a vaccinated individual receives an infection is reduced according to vaccine effectiveness.

Vaccination numbers per DZ in this study were initiated as recorded in eDRIS data, and all doses and booster doses were applied to individuals in the model, within each DZ and each age class, in the same proportions as were administered in the real population. Vaccine effectiveness in each dose phase is a fixed parameter per phase and per strain.

For the period after 11th Dec 2021, we assumed a modelled distribution of the booster doses that were being delivered at that time. We distributed booster doses to all individuals in the model, who have had their second dose, after three months (as per the actual distribution schedule at the time). We ran one scenario with 100% uptake w.r.t. 2nd dose, and one with 55% uptake. At a national level 2097633 boosters had been administered by 11 Dec 2021, 3814877 second doses had been administered by 18 Sep 2021 (12 weeks prior, thus eligible for a booster on 11 Dec 2021), thus 55% of all eligible had had their booster by 11 Dec.

More recently we also ran a final scenario based on the recorded vaccine distribution beyond the 11th December for comparison.

Based on the available information at the time [18] and consistent with other approaches [6, 7], we assume no reduction in outcome severity associated with vaccinated individuals, but rely on the transitive effect of reducing associated transmission.

Modelling COVID-19 incidence

As PHS eDRIS data gives us only the reported cases of infection, we need to determine the likely number of infected individuals with which to seed the model and to use as the summary statistic for validation and parameter estimation. For this we use the model described in Colman et al. [5] to estimate the case ascertainment ratio and thus the likely number of infected individuals over time, for the period of simulation.

Modelling transmission rate changes over time

To model the changes in activity over time—e.g those that are the effect of lockdowns, but also other more voluntary changes in behaviour—we consider two factors. First, we thin movements in the simulation (mobility reduction) in proportion to observed changes in mobility according to Google mobility reports [14]. This is applied as a proportional change in the number of individuals making between-OA movements on a given day (as above).

Second, physical distancing is incorporated via a reduction in contacts applied to both daytime and nighttime transmission rates (transmission reduction). Beyond the initial fit period (see below), we fit a change in transmission rate over time only, assuming that posterior distributions for all other parameters estimated based on the initial fit remain relevant.

Parameter estimation

Simulated epidemics are compared to the spatio-temporal pattern of COVID-19 spread in Scotland. Non-observable parameters were estimated using the incidence of COVID-19, according to the model described above, during the initial Delta-dominant period.

Estimation was performed using a Sequential Monte Carlo implementation of Approximate Bayesian Computation (ABC-SMC) [19, 15]. We calibrated the model output to the weekly incidence (number of estimated infections per week) due to COVID-19 aggregated at the level of CAs, using this spatial variation in incidence across Scotland to provide the necessary signature to properly calibrate the role of human mobility.

Simulated and observed summary statistics are compared via a score equal to a sum of squared errors, recorded weekly:

$$score = \sum_{week} \sum_{CA} (I_{sim} - I_{obs})^2$$

where I_{sim} is the weekly incidence per CA simulated and I_{obs} its observed value.

The total number of infected individuals at the start of the simulation (the seeds) are fitted as part of the inference. The seeds are randomly assigned a disease state from E , I^M , and I^S . Seed

locations are distributed according to the proportion of infections registered per Intermediate Zone on the date of the start of the simulation. Intermediate zones are *neighbourhood level* aggregates of approximately five DZs.

Uniform prior distributions constrain all parameter values to plausible ranges based on the available literature relevant to the early, pre-lockdown period. Infection dynamics are simulated via a τ -leap algorithm using half-day timesteps [20]. All parameters are listed in Table S1.

The inference framework is run on a distributed application framework (Akka) [21] running on a cloud computing infrastructure (Amazon AWS2) [22]. The model code has been written using industry grade software engineering practices including agile development for project task planning, test driven development, pair programming and code reviews to produce unit tested, robust, and reusable software components. The majority of the code has been reviewed by at least one other software developer.

Fitting transmission rate changes over time

After fitting the initial parameter set, a further temporal refinement is employed to improve the fit where the model cannot account for external factors such as changes in transmission owing to NPIs or other changes in human behaviour not captured by the mobility data. Here we perform a piece-wise least-squares fit over just the transmission rate β , per Council Area. This is piece-wise in the inflection points in the case data, which largely correspond to the times at which NPIs were enacted or relaxed.

2.3 Scoping scenarios

We modelled a range of scenarios, considering two variants (Delta and Omicron) with differing transmissibility and levels of vaccine protection. At the time of the analysis, there were limited data on the potential of the Omicron VOC for either greater transmission than the Delta VOC, or increased ability to escape either natural or vaccine-induced immunity. We therefore generated simulations over possible transmission rates and vaccine escape levels for the Omicron variant, based on this existing evidence, in order to choose combinations that generate plausible trajectories of SGTF cases in Scotland. We used values for transmission potential and vaccine efficacy from the UKHSA Technical Briefing on Variants of Concern [23].

We modelled three levels of vaccine escape: a baseline with the same vaccine efficacy as Delta (Escape Level 1), a lower vaccine escape potential (Escape Level 2) as described by the central estimates from the UKHSA Technical Briefing (90% after two doses, falling to 35% after 15 weeks, and 75% after booster), and a higher vaccine escape potential (Escape Level 3) as described by the lower efficacy bounds (65% after two doses, falling to 10% after 15 weeks, and 60% after booster).

We modelled two levels of transmissibility for Omicron: an increased level based on the UKHSA Technical Briefing estimate of $3.2\times$ household transmission, under the assumption that generalised transmission advantages, i.e. including transmission outside the household has a similar advantage, and an intermediate level based on 80% of the higher level, giving a $2.25\times$ transmission rate—corresponding with the lower bound of the UKHSA estimate. We then have two sets of scenarios. The first assumes the overall transmission rate for Delta remains at the current level. The second assumes an NPI-based intervention, reducing transmission rates to 80% its previous value on 17th December 2021, to reflect a combination of voluntary behavioural change in response to new guidance, and new restrictions. The latter scenario aims to generate a reproduction number around 0.8 for the Delta VOC, as observed during previous similar NPI restricted periods in Scotland [8]. While it is not expected that the impact of the NPIs during this period are likely to be observed in the near future, the NPI scenarios were generated to explore whether or not meaningful impacts on infection trajectories would be predicted.

We assumed that all parameters for the Omicron VOC were the same as for Delta, with the exception of the transmission rate, which was assumed to be a fixed multiplier of the transmission rates for Delta. The transmission rates for Delta are from parameters jointly drawn from the posterior parameter distributions fitted for Delta from the earlier period (i.e. from August 2021

to November 2021). Vaccine escape levels were implemented as a multiplier on the within-model vaccine efficacy for Delta as in Table 1. The combination of vaccine escape and transmission parameters generates 12 scenarios (a-l), labelled as in Table 2.

		Efficacy multiplier		
		2 dose	+15 weeks	Booster
Vaccine Escape Level	1	1	1	1
	2	1	0.45	0.8
	3	0.72	0.15	0.63

Table 1: Levels of vaccine escape used in our scenarios, with value 1 being complete protection.

The transmission model does not take account of vaccine protection from severe disease, it either completely protects individuals or fails completely and so if infected, results in an infection as likely to be severe as would be the case for infection in a previously wholly susceptible individual.

		Vaccine Escape Level		
		1	2	3
Transmission Level	1	a	b	c
	2	d	e	f
	1+NPI	g	h	i
	2+NPI	j	k	l

Table 2: Scenario labels as used in figures in the exploration of scenario plausibility.

2.4 Fitting of plausible scenarios

From the scoping scenarios, we carried forward only those that were plausible, being closest to the observed SGTF incidence trajectory. We then adjusted the transmission rates of each to fit the growth rate observed in incidence.

$$\text{Growth rate} = \frac{\ln I(t_f) - \ln I(t_0)}{t}$$

where $I(t)$ is the number of infected at time t from an initial point ($t = t_0$) fitted to match the SGTF incidence trajectory. We use the time period for which we have confirmed observed Omicron cases. We then take the growth rates for the modelled scenario (g_m) and for the observed incidence (g_o) and increase the scenario transmission rate by $\frac{g_o}{g_m}$.

We then took a range of further scenarios:

	NPI Level			
	1	2	3	4
Lower vaccine escape	m	o	q	s
Higher vaccine escape	n	p	r	t

where NPI Level 1 is as considered previously, an initial drop to 80% of the original transmission rate. Levels 2, 3, and 4 have a further post-Christmas restriction applied with a further drop to 64%, 48%, and 40% of the original transmission rates respectively, imposing these restrictions on 27th December 2021. As the mean of the fitted trajectories of the fitted Delta period were observed to stabilize after 100 runs, further simulations were restricted to this number.

3 Results

3.1 Model fit / parameters

The fit of the initial ABC-based parameter estimation to the observed data, with the resultant posterior distribution of estimated parameters is shown in Figure S2. Figure 2 shows the trajectory of incidence in the model compared to the observed data (accounting for case ascertainment), with detail at the Council Area level shown in Figure S3. Notably, the final inflection point in the piece-wise temporal transmission rate fit is at the start of October 2021, with the final inflection point in mid-November being a natural result of the modelled dynamics.

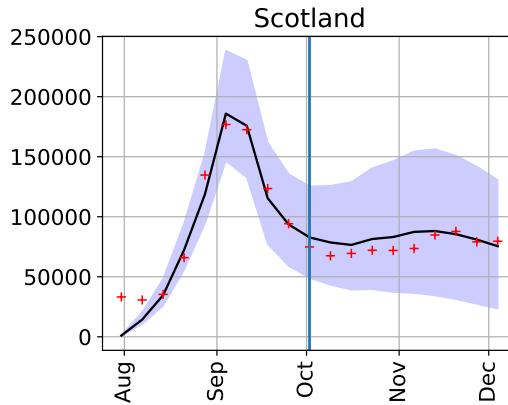


Figure 2: Model fit to observed data (incidence) for the Delta variant, after the initial ABC-based parameter estimation and temporal transmission rate fit, national scale. Vertical line shows the final inflection point in the piece-wise temporal fit.

3.2 Scoping scenario results

The dynamics of infection with respect to the Delta and Omicron variants are directly compared in Figure 3 showing trajectories both with and without NPI's in place.

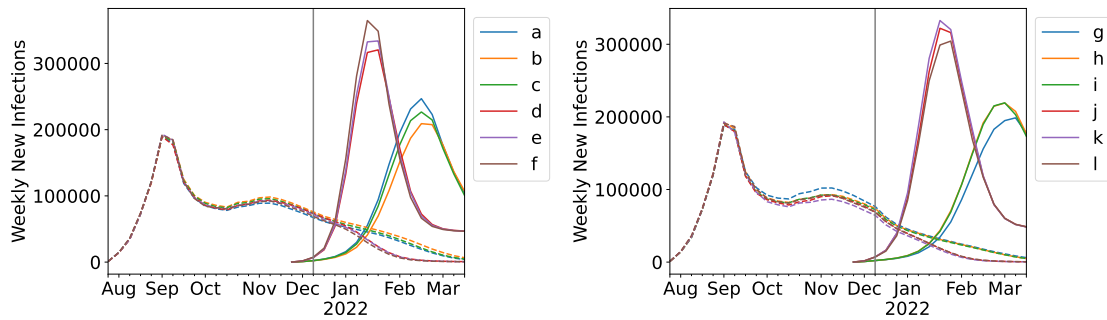


Figure 3: Comparison of scenarios with no additional NPIs (left) and additional NPIs (right). Central estimate from 200 model runs, from the vaccination distribution scheme with 55% uptake. With lower transmission rate: a-c, g-i; higher transmission rate: d-f, j-l; and increasing vaccine escape within each group. The trajectory of the Delta variant is shown as a dashed line.

Figure S4 and Figure S5 provide additional detail, showing respectively trajectories without and with further NPI's in place from 17th December, and showing the range of simulations and a comparison to the observed incidence.

3.3 Selection of plausible scenarios

We compared scenarios to the observed incidence of SGTF-only cases adjusted by our modelled case to infection ratio. Only a few scenarios, all with the higher transmission rate were close to estimating the true trajectory (growth rate) of Omicron infections (Figures S6 and S7). Hence, we restricted further scenario development to the most plausible of these.

We carry forward only scenarios k and l as being closest to the observed SGTF case trajectory, also under the assumption that the measures already in place would have had some impact. Scenario k has the lower and l the higher estimate for vaccine escape. Both have the higher transmission rate estimate. We then adjust the transmission rates of each to fit the growth rate observed in cases.

3.4 Fit scenario results

By fitting the growth rate to that of the observed Omicron cases, we achieved an initial modelled growth rate consistent with the limited knowledge of the early Omicron outbreak. Figure 4 shows the fit to observed case data (including knowledge of observed Omicron cases after 11th December that were not known at the time of original modelling).

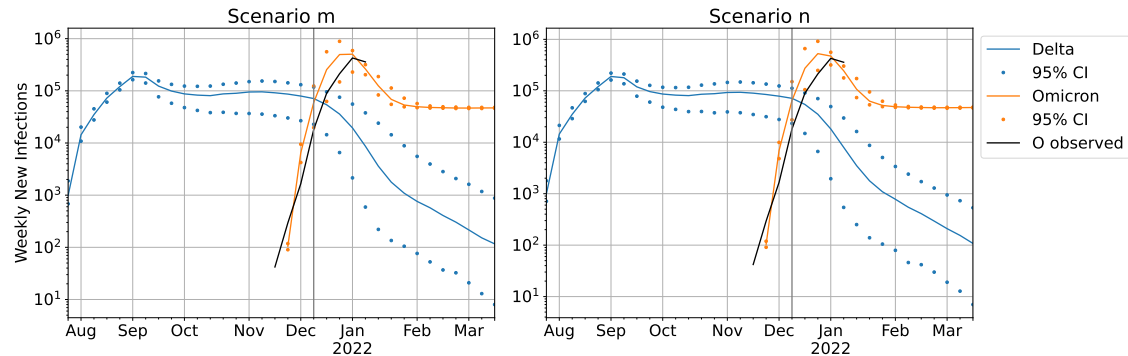


Figure 4: Adjusted transmission rate scenarios (log scale) for the 55% uptake vaccine distribution scheme: lower vaccine escape (left), higher vaccine escape (right). Dots represents bounds for 95% of 200 simulations. Observed values prior to the vertical line (11th December) were the data available at the time of fitting, used to fit the growth rate; observed values subsequent to this date were added later for comparison.

We saw little significant difference between the different strategies for forward distribution of vaccines (55% and 100% uptake of boosters with respect to the uptake of 2nd doses). Figure S8 shows in detail the effect of the different strategies, including a model with the actual uptake post-11th December for comparison.

We estimated Omicron to have a transmission rate advantage over Delta of $5.3\times$ in the lower vaccine escape scenario, and an advantage of $5.1\times$ in the higher vaccine escape scenario.

Not even the severest restrictions (a reduction of transmission rate to 40% of the rate in mid November) is there observed a significant reduction in cases, implying that restrictions alone were not likely to be sufficient to reduce the reproduction number below one. Figure 5 shows the range of post-Christmas NPI scenarios. Figure S9 details the NPI scenarios with confidence intervals.

4 Conclusions

In this study we have adapted an existing model, that was used to provide the Scottish government with medium term projections of cases of COVID-19 across Scotland over much of the “emergency” period of COVID-19 restrictions. The model was adapted to account for the transmission of two

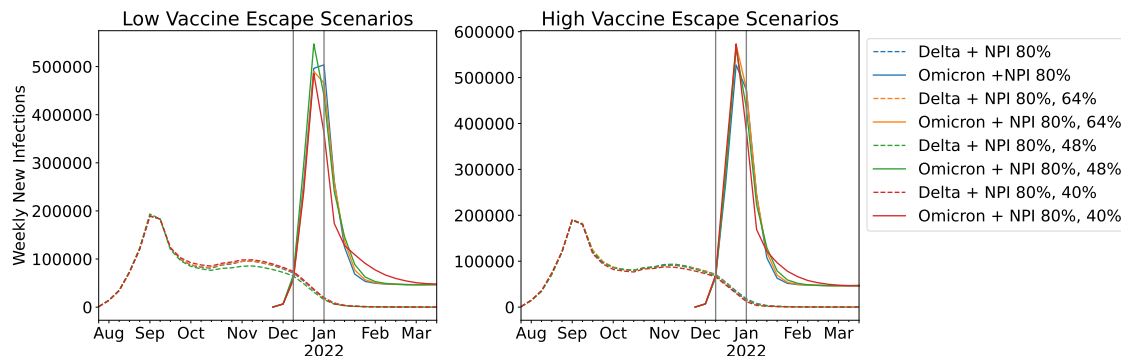


Figure 5: Adjusted transmission rate scenarios, lower vaccine escape (left), higher vaccine escape (right), with a range of post-Christmas NPI levels.

strains of SARS-CoV-2 with different levels of vaccine immune escape, in order to mimic the properties of the emergent Omicron VOC as known at time of analysis. In these models we showed that, under plausible scenarios of immune escape, only transmission rate advantages of between 5.1 and 5.3 result in trajectories consistent with the observed numbers of cases with SGTF (assumed to be the Omicron variant). While further combinations of transmission advantage and vaccine escape may of course be plausible, in our view the scenarios we examined provided a suitable backdrop on which to further investigate the impact of interventions beyond those imposed in mid-December and to provide reasonable mid-range forward projections of case numbers.

We saw little significant difference between the different strategies for forward distribution of vaccines in the model. This is most likely because the landscape of immunity already present at the time of the Omicron outbreak is much more decisive in the effect on transmission than the relatively small number of doses administered in the short period after the outbreak. Hence we consider a reasonable best estimate at projected distribution is sufficient for modelling a short to medium-term projection of infections. This would most likely not be the case for longer-term projections.

We also saw that the imposition of post-Christmas NPI restrictions that were likely to have little effect, firstly because the transmission rate advantage of the Omicron variant was so high, but also because post-Christmas the rapid outbreak would likely have already peaked meaning any restrictions at that time would likely have come too late.

One important assumption in the model was that vaccinated individuals who become infected, were as likely to experience severe disease as others. While it is known that vaccines do provide very good protection against severe infection with the Delta VOC, such data were not available at the time for the Omicron VOC. With its observed greater ability to evade vaccine induced protection, this was chosen as the more conservative option. We also assumed complete cross immunity between strains. It is known now that that this is not the case, but again there was little data available at the time to make an assessment on this.

We observe that our final adjusted scenarios remained consistent with observed Omicron cases beyond the observations available at the time of fitting. Despite assumptions, we have shown that it was possible, with a model that had been developed over the course of the Delta variant period to make a rapid and reasonable estimate of the impact of a new variant with little knowledge about its detailed dynamics. We believe this to be largely owing to the tracking of immunity throughout the population during the Delta period at fine geographical scale, and thus the model's ability to simulate the finer detail of the spatial spread of the new variant.

Looking back in comparison with observation data known now, but not yet observed at the time, we can see that the model allowed a reasonable estimate of both the scale and timing of the Omicron outbreak and the likely utility, or lack thereof, of post-Christmas NPIs. In general, we can see that the landscape of immunity prior to a variant outbreak, if it has a significant transmission

advantage, is much more important for modelling the dynamics of the initial outbreak than any shorter-term change in immunity or contact patterns after the outbreak has taken hold.

References

- [1] World Health Organisation. Classification of Omicron (B.1.1.529): SARS-CoV-2 Variant of Concern. [https://www.who.int/news/item/26-11-2021-classification-of-omicron-\(b.1.1.529\)-sars-cov-2-variant-of-concern](https://www.who.int/news/item/26-11-2021-classification-of-omicron-(b.1.1.529)-sars-cov-2-variant-of-concern), 2021.
- [2] Scottish Government. Omicron variant. <http://www.gov.scot/news/omicron-variant/>, 2021.
- [3] Juliet R. C. Pulliam, Cari van Schalkwyk, Nevashan Govender, Anne von Gottberg, Cheryl Cohen, Michelle J. Groome, Jonathan Dushoff, Koleka Mlisana, and Harry Moultrie. Increased risk of SARS-CoV-2 reinfection associated with emergence of Omicron in South Africa. *Science*, 376(6593):eabn4947, March 2022.
- [4] Christopher J. Banks, Ewan Colman, Thomas Doherty, Oliver Tearne, Mark Arnold, Katherine E. Atkins, Daniel Balaz, Gaël Beaunée, Paul R. Bessell, Jessica Enright, Adam Kleczkowski, Gianluigi Rossi, Anne-Sophie Ruget, and Rowland R. Kao. SCoVMod – a spatially explicit mobility and deprivation adjusted model of first wave COVID-19 transmission dynamics. *Wellcome Open Research*, 7:161, May 2022.
- [5] Ewan Colman, Gavril A. Puspitarani, Jessica Enright, and Rowland R. Kao. Ascertainment rate of SARS-CoV-2 infections from healthcare and community testing in the UK. *Journal of Theoretical Biology*, 558:111333, February 2023.
- [6] Rosanna C. Barnard, Nicholas G. Davies, Carl A. B. Pearson, Mark Jit, and W. John Edmunds. Projected epidemiological consequences of the Omicron SARS-CoV-2 variant in England, December 2021 to April 2022. Preprint, *Epidemiology*, December 2021.
- [7] Matt J. Keeling, Ellen Brooks-Pollock, Rob Challen, Leon Danon, Louise Dyson, Julia R. Gog, Laura Guzmán Rincón, Edward M. Hill, Lorenzo Pellis, Jonathan M. Read, and Michael J. Tildesley. Short-term Projections based on Early Omicron Variant Dynamics in England, December 2021.
- [8] Scottish Government. Coronavirus (COVID-19): Modelling the epidemic. <https://www.gov.scot/collections/coronavirus-covid-19-modelling-the-epidemic/>, 2022.
- [9] Public Health Scotland. Electronic Data Research and Innovation Service (eDRIS). <https://www.isdscotland.org/Products-and-services/Edris/>, 2022.
- [10] Scottish Government. Open access to Scotland’s official statistics. <https://statistics.gov.scot/home>, 2022.
- [11] UK Data Service. Census Support: Flow Data. <https://wicid.ukdataservice.ac.uk/>, 2022.
- [12] National Records of Scotland. 2011 census: Geographies. <https://www.scotlandscensus.gov.uk/about/2011-census/2011-census-geographies/>, 2022.
- [13] Scottish Government. Scottish Index of Multiple Deprivation 2020. <https://www.gov.scot/collections/scottish-index-of-multiple-deprivation-2020/>, 2022.
- [14] Google Inc. COVID-19 Community Mobility Report. <https://www.google.com/covid19/mobility?hl=en>, 2022.
- [15] Tina Toni, David Welch, Natalja Strelkowa, Andreas Ipsen, and Michael P.H. Stumpf. Approximate Bayesian computation scheme for parameter inference and model selection in dynamical systems. *Journal of the Royal Society Interface*, 6(31):187–202, 2009.

- [16] Alex Arenas, Wesley Cota, Jesus Gomez-Gardenes, Sergio Gómez, Clara Granell, Joan Matalas, David Soriano-Panos, and Benjamin Steinegger. A mathematical model for the spatiotemporal epidemic spreading of COVID19. *MedRxiv*, 2020.
- [17] Laura Di Domenico, Giulia Pullano, Chiara E. Sabbatini, Pierre Yves Boëlle, and Vittoria Colizza. Impact of lockdown on COVID-19 epidemic in Île-de-France and possible exit strategies. *BMC Medicine*, 18(1):1–13, 2020.
- [18] Nick Andrews, Julia Stowe, Freja Kirsebom, Samuel Toffa, Tim Rickeard, Eileen Gallagher, Charlotte Gower, Meaghan Kall, Natalie Groves, Anne-Marie O’Connell, David Simons, Paula B. Blomquist, Asad Zaidi, Sophie Nash, Nurin Iwani Binti Abdul Aziz, Simon Thelwall, Gavin Dabrera, Richard Myers, Gayatri Amirthalingam, Saheer Gharbia, Jeffrey C. Barrett, Richard Elson, Shamez N Ladhani, Neil Ferguson, Maria Zambon, Colin NJ Campbell, Kevin Brown, Susan Hopkins, Meera Chand, Mary Ramsay, and Jamie Lopez Bernal. Effectiveness of COVID-19 vaccines against the Omicron (B.1.1.529) variant of concern. Preprint, *Epidemiology*, December 2021.
- [19] Florian Hartig, Justin M. Calabrese, Björn Reineking, Thorsten Wiegand, and Andreas Huth. Statistical inference for stochastic simulation models - theory and application. *Ecology Letters*, 14(8):816–827, 2011.
- [20] D. T. Gillespie. Approximate accelerated stochastic simulation of chemically reacting systems. *Journal of Chemical Physics*, 115(4):1716–1733, 2001.
- [21] Lightbend Inc. Akka: Build concurrent, distributed, and resilient message-driven applications for Java and Scala. <https://akka.io/>, 2022.
- [22] Amazon Web Services Inc. Cloud Computing Services - Amazon Web Services (AWS). <https://aws.amazon.com/>, 2022.
- [23] UK Health Security Agency. SARS-CoV-2 variants of concern and variants under investigation: Technical briefing 31. Technical report, UK Health Security Agency, 2021.
- [24] Xi He, Eric H.Y. Lau, Peng Wu, Xilong Deng, Jian Wang, Xinxin Hao, Yiu Chung Lau, Jessica Y. Wong, Yujuan Guan, Xinghua Tan, Xiaoneng Mo, Yanqing Chen, Baolin Liao, Weilie Chen, Fengyu Hu, Qing Zhang, Mingqiu Zhong, Yanrong Wu, Lingzhai Zhao, Fuchun Zhang, Benjamin J. Cowling, Fang Li, and Gabriel M. Leung. Temporal dynamics in viral shedding and transmissibility of COVID-19. *Nature Medicine*, 26(5):672–675, 2020.
- [25] Ruiyun Li, Sen Pei, Bin Chen, Yimeng Song, Tao Zhang, Wan Yang, and Jeffrey Shaman. Substantial undocumented infection facilitates the rapid dissemination of novel coronavirus (SARS-CoV-2). *Science*, 368(6490):489–493, 2020.
- [26] Qifang Bi, Yongsheng Wu, Shujiang Mei, Chenfei Ye, Xuan Zou, Zhen Zhang, Xiaojian Liu, Lan Wei, Shaun A. Truelove, Tong Zhang, Wei Gao, Cong Cheng, Xiujuan Tang, Xiaoliang Wu, Yu Wu, Binbin Sun, Suli Huang, Yu Sun, Juncen Zhang, Ting Ma, Justin Lessler, and Tiejian Feng. Epidemiology and transmission of COVID-19 in 391 cases and 1286 of their close contacts in Shenzhen, China: A retrospective cohort study. *The Lancet Infectious Diseases*, 20(8):911–919, 2020.
- [27] Juanjuan Zhang, Maria Litvinova, Wei Wang, Yan Wang, Xiaowei Deng, Xinghui Chen, Mei Li, Wen Zheng, Lan Yi, Xinhua Chen, Qianhui Wu, Yuxia Liang, Xiling Wang, Juan Yang, Kaiyuan Sun, Ira M. Longini, M. Elizabeth Halloran, Peng Wu, Benjamin J. Cowling, Stefano Merler, Cecile Viboud, Alessandro Vespignani, Marco Ajelli, and Hongjie Yu. Evolving epidemiology and transmission dynamics of coronavirus disease 2019 outside Hubei province, China: A descriptive and modelling study. *The Lancet Infectious Diseases*, 20(7):793–802, 2020.

- [28] Natalie Linton, Tetsuro Kobayashi, Yichi Yang, Katsuma Hayashi, Andrei Akhmetzhanov, Sung-mok Jung, Baoyin Yuan, Ryo Kinoshita, and Hiroshi Nishiura. Incubation Period and Other Epidemiological Characteristics of 2019 Novel Coronavirus Infections with Right Truncation: A Statistical Analysis of Publicly Available Case Data. *Journal of Clinical Medicine*, 9(2):538, 2020.
- [29] Stephen A. Lauer, Kyra H. Grantz, Qifang Bi, Forrest K. Jones, Qulu Zheng, Hannah R. Meredith, Andrew S. Azman, Nicholas G. Reich, and Justin Lessler. The incubation period of coronavirus disease 2019 (CoVID-19) from publicly reported confirmed cases: Estimation and application. *Annals of Internal Medicine*, 172(9):577–582, 2020.
- [30] Steven Sanche, Yen Ting Lin, Chonggang Xu, Ethan Romero-Severson, Nicolas W. Hengartner, and Ruian Ke. The novel coronavirus, 2019-nCoV, is highly contagious and more infectious than initially estimated. *arXiv*, 2020.
- [31] Steven Sanche, Yen Ting Lin, Chonggang Xu, Ethan Romero-Severson, Nick Hengartner, and Ruian Ke. High Contagiousness and Rapid Spread of Severe Acute Respiratory Syndrome Coronavirus 2. *Emerging Infectious Diseases*, 26(7):1470–1477, 2020.
- [32] Dawei Wang, Bo Hu, Chang Hu, Fangfang Zhu, Xing Liu, Jing Zhang, Binbin Wang, Hui Xiang, Zhenshun Cheng, Yong Xiong, Yan Zhao, Yirong Li, Xinghuan Wang, and Zhiyong Peng. Clinical Characteristics of 138 Hospitalized Patients with 2019 Novel Coronavirus-Infected Pneumonia in Wuhan, China. *JAMA - Journal of the American Medical Association*, 323(11):1061–1069, 2020.
- [33] Tao Liu, Jianxiong Hu, Jianpeng Xiao, Guan hao He, Min Kang, Zuhua Rong, Lifeng Lin, Haojie Zhong, Qiong Huang, Aiping Deng, Weilin Zeng, Xiaohua Tan, Siqing Zeng, Zhihua Zhu, Jiansen Li, Dexin Gong, Donghua Wan, Shaowei Chen, Lingchuan Guo, Yan Li, Limei Sun, Wenjia Liang, Tie Song, Jianfeng He, and Wenjun Ma. Time-varying transmission dynamics of Novel Coronavirus Pneumonia in China. *bioRxiv*, 2020.
- [34] Ya nan Han, Zhan wei Feng, Li na Sun, Xiao xia Ren, Hua Wang, Yong ming Xue, Yi Wang, and Ying Fang. A comparative-descriptive analysis of clinical characteristics in 2019-coronavirus-infected children and adults. *Journal of Medical Virology*, 92(9):1596–1602, 2020.
- [35] Rachael Pung, Calvin J. Chiew, Barnaby E. Young, Sarah Chin, Mark I.C. Chen, Hannah E. Clapham, Alex R. Cook, Sebastian Maurer-Stroh, Matthias P.H.S. Toh, Cuiqin Poh, Mabel Low, Joshua Lum, Valerie T.J. Koh, Tze M. Mak, Lin Cui, Raymond V.T.P. Lin, Derrick Heng, Yee Sin Leo, David C. Lye, Vernon J.M. Lee, Kai qian Kam, Shirin Kalimuddin, Seow Yen Tan, Jiashen Loh, Koh Cheng Thoon, Shawn Vasoo, Wei Xin Khong, Nur Afidah Suhaimi, Sherlynn JH Chan, Emma Zhang, Olivia Oh, Albert Ty, Charlene Tow, Yi Xian Chua, Wei Liang Chaw, Yixiang Ng, Farid Abdul-Rahman, Shafiq Sahib, Zheng Zhao, Cheryl Tang, Constance Low, Ee Hui Goh, Georgina Lim, Yan’an Hou, Imran Roshan, James Tan, Kelly Foo, Khine Nandar, Lalitha Kurupatham, Pei Pei Chan, Pream Raj, Yijun Lin, Zubaidah Said, Anne Lee, Cherie See, Jessey Markose, Joanna Tan, Guan hao Chan, Wanhan See, Xinyi Peh, Vincent Cai, Wen Kai Chen, Zongbin Li, Roy Soo, Angela LP Chow, Wycliffe Wei, Aysha Farwin, and Li Wei Ang. Investigation of three clusters of COVID-19 in Singapore: Implications for surveillance and response measures. *The Lancet*, 395(10229):1039–1046, 2020.
- [36] Robert Verity, Lucy C. Okell, Ilaria Dorigatti, Peter Winskill, Charles Whittaker, Natsuko Imai, Gina Cuomo-Dannenburg, Hayley Thompson, Patrick G.T. Walker, Han Fu, Amy Dighe, Jamie T. Griffin, Marc Baguelin, Sangeeta Bhatia, Adhiratha Boonyasiri, Anne Cori, Zulma Cucunubá, Rich FitzJohn, Katy Gaythorpe, Will Green, Arran Hamlet, Wes Hinsley, Daniel Laydon, Gemma Nedjati-Gilani, Steven Riley, Sabine van Elsland, Erik Volz, Haowei

Wang, Yuanrong Wang, Xiaoyue Xi, Christl A. Donnelly, Azra C. Ghani, and Neil M. Ferguson. Estimates of the severity of coronavirus disease 2019: A model-based analysis. *The Lancet Infectious Diseases*, 20(6):669–677, 2020.

- [37] Ana Da Silva Filipe, James Shepherd, Thomas Williams, Joseph Hughes, Elihu Aranday-Cortes, Patawee Asamaphan, Carlos Balcazar, Kirstyn Brunner, Stephen Carmichael, Rebecca Dewar, Michael Gallagher, Rory Gunson, Antonia Ho, Natasha Jesudason, Natasha Johnson, E. Carol McWilliam Leitch, Kathy Li, Alasdair MacLean, Daniel Mair, Sarah McDonald, Martin McHugh, Jenna Nichols, Marc Niebel, Kyriaki Nomikou, Richard Orton, Aine O’Toole, Massimo Palmarini, Yasmin Parr, Andrew Rambaut, Stefan Rooke, Sharif Shaaban, Rajiv Shah, Joshua Singer, Katherine Smollett, Igor Starinskij, Lily Tong, Vattipally Sreenu, Elizabeth Wastnedge, David Robertson, Matthew Holden, Kate Templeton, and Emma Thomson. Genomic epidemiology of SARS-CoV-2 spread in Scotland highlights the role of European travel in COVID-19 emergence. *medRxiv*, 2020.
- [38] Jing Qin, Chong You, Qiushi Lin, Taojun Hu, Shicheng Yu, and Xiao Hua Zhou. Estimation of incubation period distribution of COVID-19 using disease onset forward time: A novel cross-sectional and forward follow-up study. *Science Advances*, 6(33):1–7, 2020.
- [39] Matt Arentz, Eric Yim, Lindy Klaff, Sharukh Lokhandwala, Francis X. Riedo, Maria Chong, and Melissa Lee. Characteristics and Outcomes of 21 Critically Ill Patients with COVID-19 in Washington State. *JAMA - Journal of the American Medical Association*, 323(16):1612–1614, 2020.

Supplementary Figures

Within each OA i the infection process is governed by the frequency dependent force of infection at time t :

$$\Lambda_i(t) = - \left[(\beta_N + \beta_D) \sum_{a \in Y, E} (yI_{ia}^M + I_{ia}^S) + \beta_N (yI_{ia}^M + I_{ia}^S) + \beta_D I_{ia}^S \right. \\ \left. + \beta_D \left\{ \left\{ \sum_j (1 - \sum_j x_{ij})(yI_{ia}^M) \right\} \right. \right. \\ \left. \left. + \sum_j \left\{ x_{ij} \left(\sum_k (1 - x_{jk})(yI_{ja}^M) + I_{ja}^S + \sum_{a \in Y, E} (yI_{ja}^M + I_{ja}^S) \right) \right\} \right\} \right] / N_i$$

where:

- β_N and β_D are the nighttime and daytime transmission rates,
- $a \in \{Y, A, E\}$ is the age class (Young, Adult, Elderly),
- y is the transmission rate modifier for mildly infected individuals,
- I_{ia}^M is the number of mildly infected at location i in age class a ,
- I_{ia}^S is the number of severely infected at location i in age class a ,
- x_{ij} is the proportion of individuals commuting between locations i and j ,
- N_i is the population of location i .

Figure S1: Equation: Force of infection for location i at time t .

Parameter	Transition	Symbol	Age	Value	Prior	References
Latency period	$E \rightarrow I^M$	$1/\gamma$	All	fitted	U(1.67,28)	[16, 24, 25, 26, 27]
Days from mild infectiousness to recovery	$I^M \rightarrow R$	$1/\rho_M$	All	fitted	U(0.67,28)	[17, 27]
Symptom onset time after infectiousness	$I^M \rightarrow I^S$	$1/\gamma_M$	All	fitted	U(2,28)	[16, 24, 25, 26, 27, 28, 29, 30, 31]
Transmission rate for severe infectors (baseline, daytime)	$S \rightarrow E$	β_d	All	fitted	U(0,6)	
Transmission rate for severe infectors (baseline, nighttime)	$S \rightarrow E$	β_n	All	fitted	U(0,6)	
Transmission rate multiplier for mild infectors	$S \rightarrow E$	y	All	fitted	U(0,2.6)	
Severe symptom onset to hospitalization	$I^S \rightarrow H$	$1/\eta$	All	4		[30, 31, 32, 33, 34, 35, 36, 37]
Severe symptom onset to recovery for non-hospitalised	$I^S \rightarrow R$	$1/\rho_S$	Young Adults Elderly	19 20.7 21.6		[30]
Days hospitalisation to death	$H \rightarrow D$	$1/\mu_H$	Young Adults Elderly	6.97 6.62		eDRIS data eDRIS data eDRIS data
Proportion of hospitalised who recover	$H \rightarrow R$	$\rho_H/(\rho_H + \mu_H)$	Young Adults Elderly	1 0.96 0.84		eDRIS data eDRIS data eDRIS data
Symptoms onset to death	$I^S \rightarrow D$	$1/\mu_S$	Adults	16		[31, 38, 33, 39, 37, 36]
Mortality rate multiplier (relative to average health index)		μ_{mod}	All	fitted	U(0,0.08)	
Number of seed infections (Delta variant)		N_s	N/A	fitted	U(10, 20000)	
Number of seed recovered individuals (Delta variant)		N_R	N/A	fitted	U(2m, 5m)	

Table S1: Epidemiological parameters in SCoVMod, with priors and fixed values as appropriate. Where age is not indicated, parameters are assumed to be age independent. All times are measured in days.

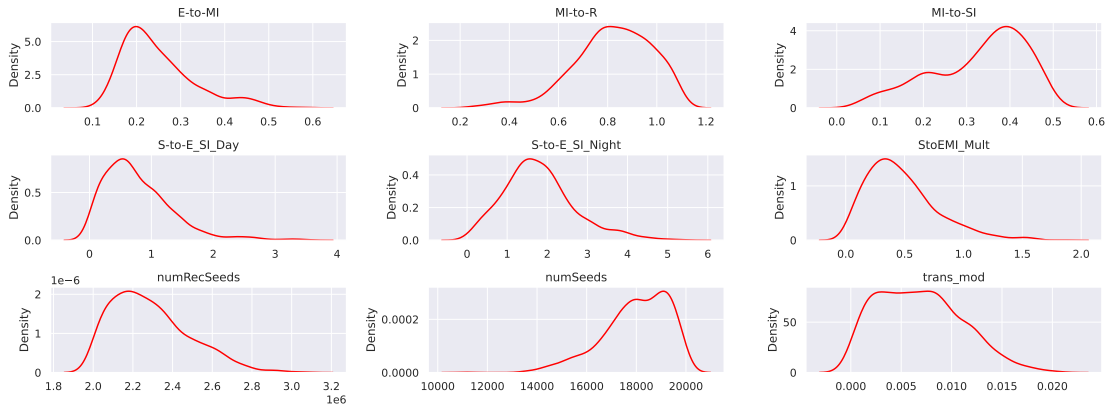


Figure S2: Posterior distribution of parameters, as a result of the initial ABC-based parameter estimation.

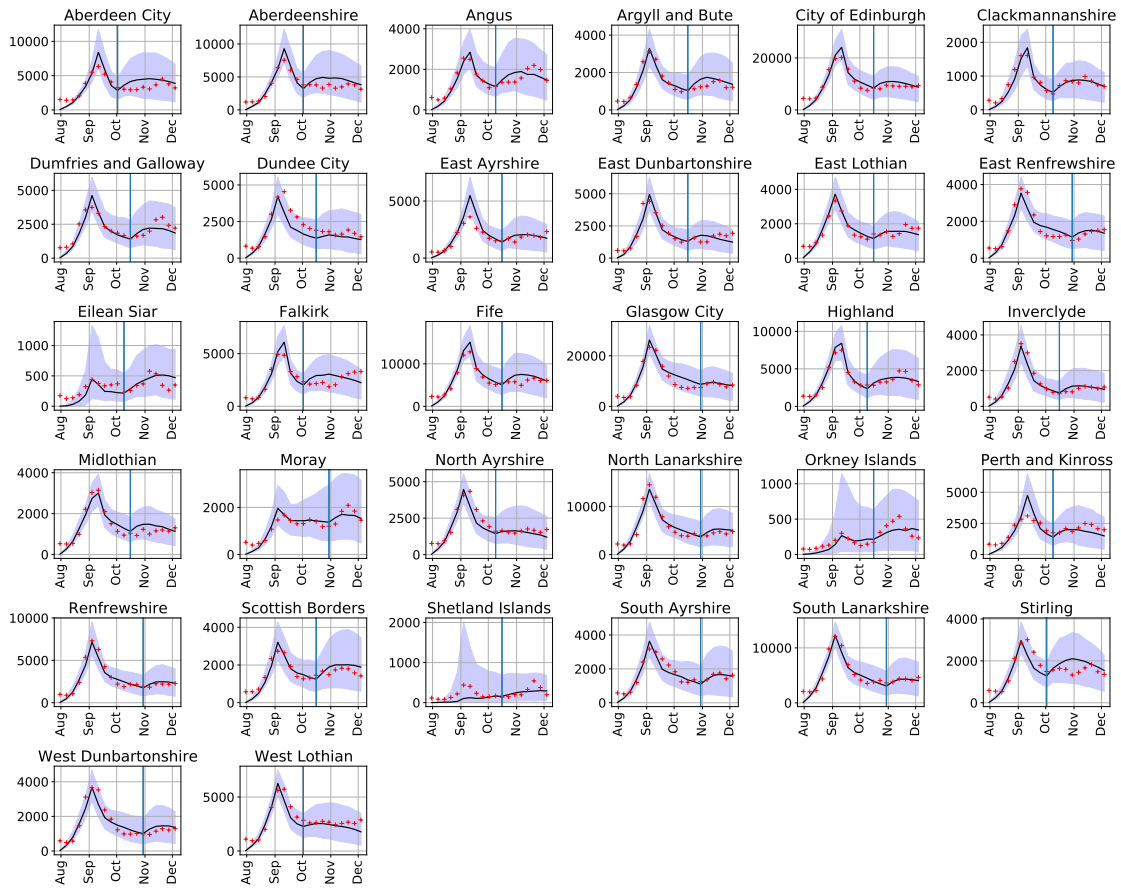


Figure S3: Council Area breakdown of the model fit to observed data, after the initial ABC-based parameter estimation and temporal transmission rate fit.

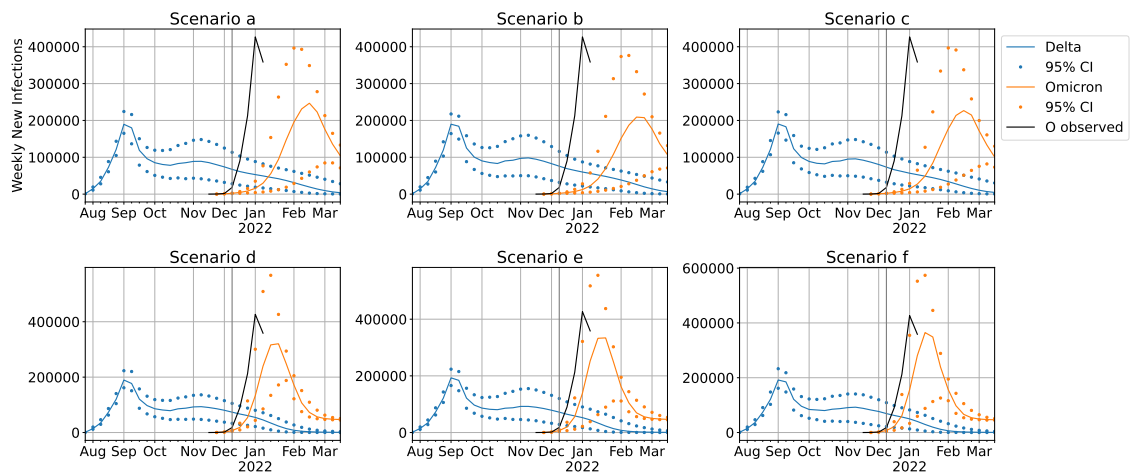


Figure S4: Scoping scenarios with increasing vaccine escape from left to right, increasing Omicron transmission rate from top to bottom. 55% uptake vaccine distribution scheme.

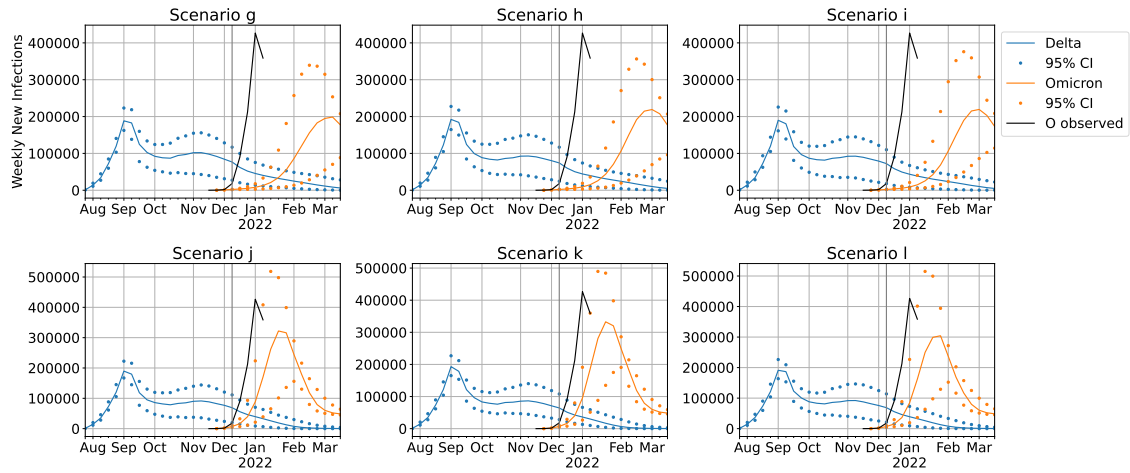


Figure S5: Scoping scenarios with additional NPI reducing transmission rates to 80%: increasing vaccine escape from left to right, increasing Omicron transmission rate from top to bottom. 55% uptake vaccine distribution scheme.

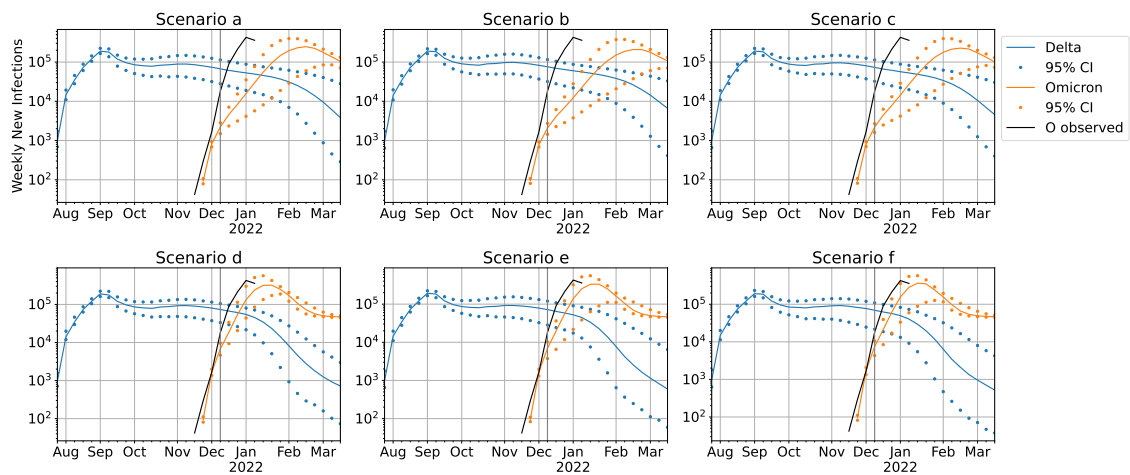


Figure S6: Scoping scenarios with increasing vaccine escape from left to right, increasing Omicron transmission rate from top to bottom. 55% uptake vaccine distribution scheme. (Log scale.)

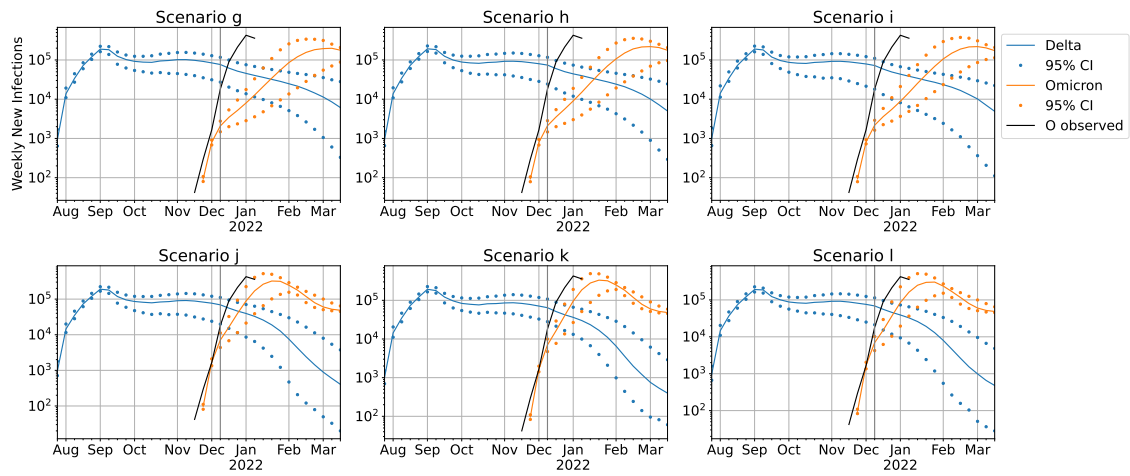


Figure S7: Scoping scenarios with additional NPI reducing transmission rates to 80%: increasing vaccine escape from left to right, increasing Omicron transmission rate from top to bottom. 55% uptake vaccine distribution scheme. (Log scale.)

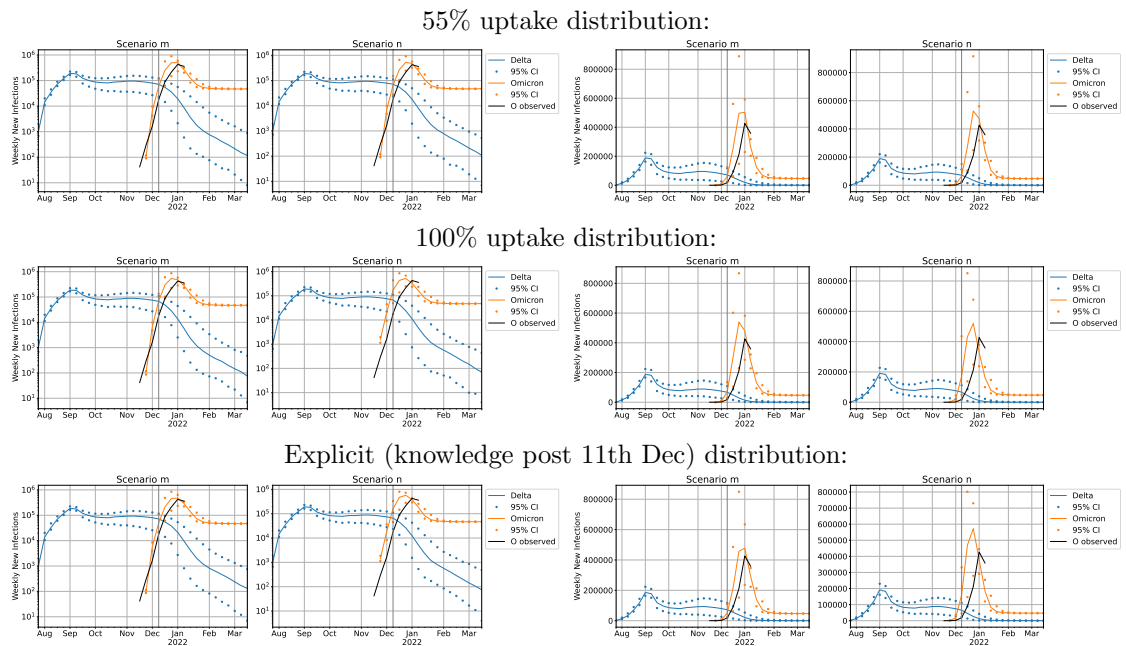


Figure S8: Adjusted transmission rate scenarios (log scale left, linear scale right) for each vaccine distribution scheme with lower vaccine escape (left of each pair) and higher vaccine escape (right of each pair). Dots represents bounds for 95% of 200 simulations. Observed values prior to the vertical line (11th December) were the data available at the time of fitting, used to fit the growth rate; observed values subsequent to this date were added later for comparison.

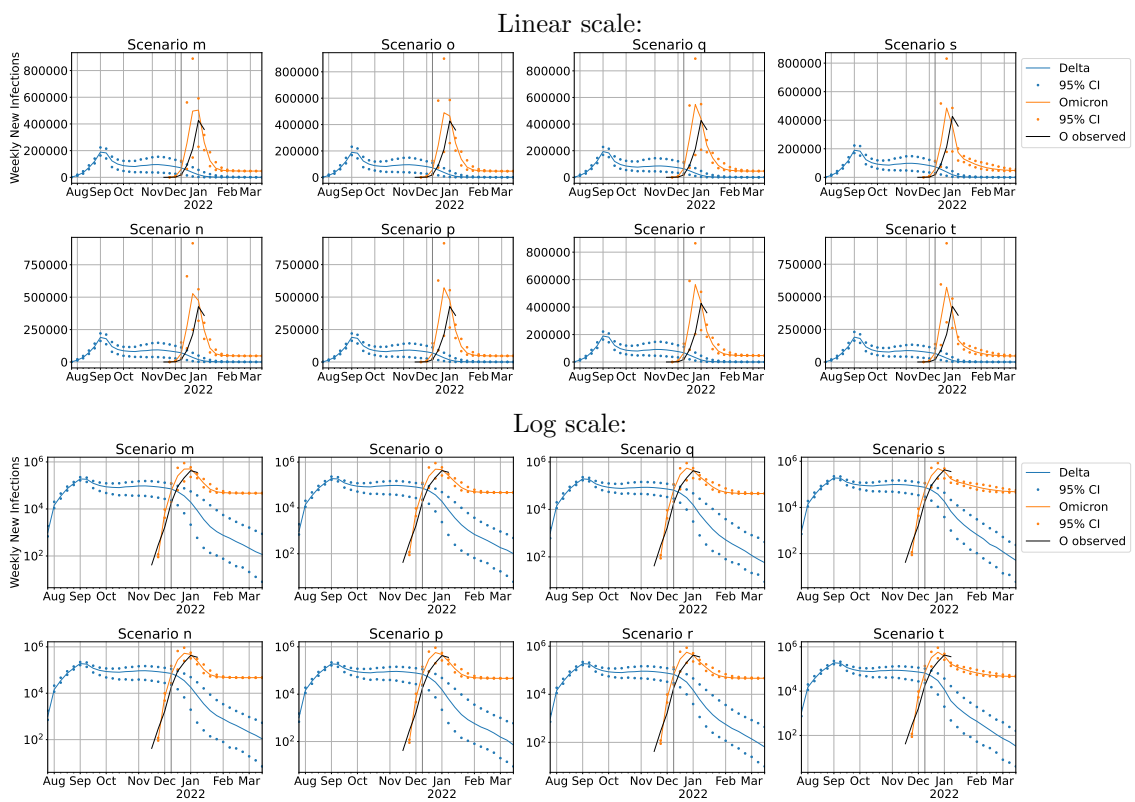


Figure S9: NPI adjusted transmission rate scenarios with 55% uptake vaccine distribution scheme.

For the purpose of open access, the author has applied a Creative Commons Attribution (CC BY) licence to any Author Accepted Manuscript version arising from this submission.